HHS Public Access

Author manuscript

Cerebellum. Author manuscript; available in PMC 2024 February 09.

Published in final edited form as:

Cerebellum. 2022 October ; 21(5): 801–813. doi:10.1007/s12311-022-01382-8.

The Primary Ciliary Deficits in Cerebellar Bergmann Glia of the Mouse Model of Fragile X Syndrome

Bumwhee Lee[*],

Laura Beuhler[*],

Hye Young Lee[**]

The Department of Cellular and Integrative Physiology; the University of Texas Health Science Center at San Antonio; San Antonio, Texas, 78229; USA

Abstract

Primary cilia are non-motile cilia that function as antennae for cells to sense signals. Deficits of primary cilia cause ciliopathies, leading to the pathogenesis of various developmental disorders; however, the contribution of primary cilia to neurodevelopmental disorders is largely unknown. Fragile X syndrome (FXS) is a genetically inherited disorder and the most common known cause for autism spectrum disorders. FXS is caused by the silencing of the fragile X mental retardation 1 (*FMR1*) gene, which encodes for the fragile X mental retardation protein (FMRP). Here, we discovered a reduction in primary cilia number and Sonic hedgehog (Shh) signaling in cerebellar Bergmann glia of *Fmr1* KO mice. We further found reduced granule neuron precursor (GNP) proliferation and thickness of the external germinal layer (EGL) in *Fmr1* KO mice, implicating that primary ciliary deficits in Bergmann glia may contribute to cerebellar developmental phenotypes in FXS, as Shh signaling through primary cilia in Bergmann glia is known to mediate proper GNP proliferation in the EGL. Taken together, our study demonstrates that FMRP loss leads to primary cilia deficits in cerebellar Bergmann glia which may contribute to cerebellar deficits in FXS.

Keywords

Primary cilia; fragile X syndrome; FMRP; cerebellum; Bergmann glia

Introduction

The primary cilium is a specialized organelle found in most mammalian cell types that grows from basal bodies and extends from the cell surface. The primary cilium is present in multiple cell types in the brain, including neurons and glia, and mediates numerous signal

[**]Correspondence: Hye Young Lee, Leeh6@uthscsa.edu.

[*] These authors contributed equally

Author Contributions

B.L. and L.B. conceived the study, performed the experiments, and wrote the manuscript. H.Y.L. supervised the whole project and wrote the manuscript.

Declaration of Interests

The authors declare no competing interests.

transduction pathways, such as the Sonic hedgehog (Shh), Wnt, Notch, Hippo, mammalian target of rapamycin (mTOR), G-protein coupled receptor (GPCR), and platelet-derived growth factor receptor a (PDGFRa) (Veland et al., 2009; Wheway et al., 2018). Deficits of primary cilia, in function or formation, cause ciliopathies leading to the pathogenesis of various developmental disorders and diseases in humans (Badano et al., 2006; Lee and Gleeson, 2010; Ware et al., 2011) and often show brain phenotypes such as mental retardation and cognitive defects (Badano et al., 2006). As Shh signaling is critical for early neurodevelopment, ablation of critical proteins which form primary cilia, including various intraflagellar transport (IFT) or IFT-associated proteins such as IFT88 and Kif3a, lead to defects in embryonic patterning and development (Huangfu et al., 2003). Defects in primary cilia or their associated IFT proteins are also known to lead to severe cerebellar deficits (Chizhikov et al., 2007; Spassky et. al. 2008). In the postnatal brain, granule neuron precursors (GNPs) require primary cilia for proliferation and differentiation in multiple brain regions including the cerebellum (Chizhikov et al., 2007; Di Pietro et al., 2017; Spassky et al., 2008) and the dentate gyrus (Breunig et al., 2008; Han et al., 2008). It has been shown that cooperation between Shh signaling and Atoh1, which mainly expresses in proliferating GNPs in the external germinal layer (EGL) of the cerebellum, a region important during early postnatal cerebellar development and controls primary cilia maintenance and function, orchestrate proper GNP development in the cerebellum (Chang et al., 2019; Flora et al., 2009). Moreover, studies further demonstrate that glia-neuronal coordination and communication is also crucial for maintaining a proper neuronal number and normal cerebellar development. The ablation of Shh signaling in Bergmann glia, a type of astrocyte residing in the Purkinje cell layer (PCL), leads to proliferation deficits in early stages of cerebellar development by affecting the proliferation of cerebellar GNPs in the EGL (Cheng et al., 2018; Marazziti et al., 2013), which would eventually differentiate into granule neurons and migrate to the internal granule layer (IGL), guided by the Bergmann glia (Xu et al., 2013). Furthermore, the loss of the primary cilia protein Gpr37l1, which specifically expresses in Bergmann glia, has led to reduced Shh signaling, reduced GNP proliferation in the EGL, and the alteration of cerebellum-mediated behaviors including motor coordination (Marazziti et al., 2013). These granule neurons produced in the EGL are important for a variety of tasks in the cerebellum, such as pruning the climbing fibers which synapse with Purkinje cells and processing both sensory and motor signals (Huang et al., 2013; Lackey et al., 2018; Manzini et al., 2006; Watanabe and Kano, 2011). Notably, granule neurons play a key role in motor learning by forming synapses with mossy fibers (Huang et al., 2013) and assisting with conditioned responses to stimuli (Giovannucci et al., 2017). Even though primary cilia play a critical role in cerebellum development, the contribution of primary cilia to neurodevelopmental disorders such as autism spectrum disorder (ASD), which often demonstrate deficits in cerebellar development, is largely unknown.

Fragile X syndrome (FXS), the most common known cause for ASDs, is a genetically inherited neurodevelopmental disorder driven by the silencing of the fragile X mental retardation 1 (*FMR1*) gene. The *FMR1* gene encodes for the fragile X mental retardation protein (FMRP), which is an mRNA binding protein and plays critical roles in regulating FMRP mRNA targets in neurons (Antar et al., 2004; Bakker et al., 2000; Cook et

al., 2011; Feng et al., 1997, Laggerbauer et al., 2001). FXS patients have a range of neurodevelopmental deficits, such as cognitive impairment and intellectual disabilities, and also display cerebellar phenotypes, such as cerebellar ataxia, decreased cerebellar size, and speech articulation deficits (Bardoni et al., 2006; Greco et al., 2011; O'Donnell and Warren, 2002). *Fmr1* KO mice, a model to study FXS, recapitulate human behavioral phenotypes including cerebellar deficits, such as abnormalities in motor coordination and balance, and deficits in rhythmic oromotor coordination (Roy et al., 2011). Deficits in mouse eyeblink conditioning behavior, mediated by the cerebellum, were also observed when FMRP was conditionally knocked out in the Purkinje cells of the cerebellum, indicating that the altered plasticity or function of the cerebellum contributes to FXS phenotypes (Koekkoek et. al. 2005). Similar deficits such as impaired cerebellar development and patterning are also found in other neurodevelopmental disorders such as Joubert syndrome and Bardet-Biedel syndrome (Aksoy et al., 2011; Mancini et al., 2014; Parisi, 2019; Valente et al., 2014). Both of these disorders are coined as 'ciliopathies', as they are caused by deficits in primary cilia or their associated proteins (Waters and Beales, 2011). Due to the similarities between the neurodevelopmental deficits of FXS and ciliopathies, the possible contribution of primary cilia in FXS pathophysiology has been raised. Notably, our previous study shows a link between FXS and primary cilia, as we found primary cilia deficits in newborn neurons of the dentate gyrus in *Fmr1* KO mice (Lee et al., 2020). Therefore, investigating further whether primary cilia contribute to the pathophysiology of FXS can be important in understanding this disorder.

This study pursued finding a phenotype of primary cilia in the cerebellum using *Fmr1* KO mice. The initial investigation assessed the number of primary cilia in different regions of the cerebellum (anterior, central, and posterior) in the PCL and the IGL of WT and *Fmr1* KO adult mice. Reduced numbers of primary cilia in the *Fmr1* KO mice were observed in location-specific, age-specific, and cell type-specific manners in that only Bergmann glia in the PCL of the posterior cerebellum showed primary cilia deficits after postnatal day 10 (P10). We further observed the reduction of Gli1 expression, an indicator of Shh signaling in Bergmann glia, and the reduction of GNP proliferation and thickness in the EGL of *Fmr1* KO mice without observing a change in primary cilia number in the EGL. Given that Shh signaling occurs in the cerebellum during proliferation and that ablation or reduction of Shh signaling in Bergmann glia leads to proliferation deficits of the cerebellar GNPs in the EGL (Cheng et al., 2018; Marazziti et al., 2013), our results indicate that dysregulated Shh signaling in Bergmann glia through primary cilia in *Fmr1* KO mice may have led to the reduced proliferation of GNPs and, therefore, the reduced thickness of the EGL observed. Taken together, we demonstrate that FMRP is required for primary cilia on the Bergmann glia for proper development of the cerebellum through glia-neuronal communication.

Materials and Methods

Materials.

Paraformaldehyde (PFA) and D(+)-Sucrose were purchased from Acros Organics. Sodium citrate dihydrate, Triton-X 100, phosphate buffered saline (PBS), Tissue-Plus® O.C.T. Compound, Permount Mounting Medium, and Superfrost Plus microscope slides were

purchased from Fisher Scientific. The X-Gal Staining Kit for β-gal staining was purchased from Genlantis. Isoflurane was purchased from Vetone. Embedding molds were purchased from Epredia. Goat serum was purchased from Gibco. BrdU, Prolong Gold Antifade Reagent, and DAPI were purchased from Invitrogen. Nuclear Fast Red solution was purchased from Sigma-Aldrich.

Antibodies.

The following primary antibodies were used in this study: mouse anti-BLBP (1:200; Abcam; ab131137), mouse anti-Sox-2 (1:100; Santa Cruz; sc-365964), mouse anti-S-100β chain (1:100; Santa Cruz; sc-393919), mouse anti-NeuN (1:500; Millipore-Sigma; MAB-377), chicken anti-calbindin (1:400; Encor; CPCA-Calbindin), rabbit anti-Arl13b (1:700; Proteintech; 17711–1-AP), rabbit anti-BLBP (1:300; Abcam; ab32423), rat anti-BrdU (1:200; Novus; NB500–169), and rat anti-BrdU (1:200; Abcam; ab6326). The following secondary antibodies were used in this study: donkey anti-mouse IgG-Alexa Fluor 647 (1:500), donkey anti-rabbit IgG-Cy3 (1:500), donkey anti-chicken IgG-Alexa Fluor 647 (1:500), donkey anti-chicken IgG-Cy2 (1:500), and donkey anti-rat IgG-Alexa Fluor 488 (1:200) from Jackson ImmunoResearch Laboratories.

Animals.

FVB.129P2-*Pde6b*$^{+}$ *Tyr*$^{c\text{-}ch}$*Fmr1*^{tm1Cgr}/J (FVB *Fmr1* KO; JAX: #004624), FVB.129P2-*Pde6b*$^{+}$ *Tyr*$^{c\text{-}ch}$/AntJ (FVB control mice for *Fmr1* KO; JAX: #004828), and *Gli1*^{tm2Alj}/J (Gli1-*lacZ*; JAX: #008211) mice were purchased from Jackson Laboratory. FVB *Fmr1* KO males (*Fmr1*$^{-/y}$) were crossed with control females (*Fmr1*$^{+/+}$) to obtain heterozygous *Fmr1* females (*Fmr1*$^{+/-}$), which were then crossed with control males (*Fmr1*$^{+/y}$) to obtain male *Fmr1* KO mice (*Fmr1*$^{-/y}$) and male control WT littermates (*Fmr1*$^{+/y}$). For Gli1-*lacZ* experiments, heterozygous FVB *Fmr1* females (*Fmr1*$^{+/-}$) were crossed with heterozygous Gli1-*lacZ* males (Gli1-*lacZ*$^{+/-}$) to obtain male Gli1-*lacZ*;*Fmr1* KO mice (Gli1-*lacZ*$^{+/-}$,*Fmr1*$^{-/y}$) and male Gli1-*lacZ*;WT control littermates (Gli1-*lacZ*$^{+/-}$;*Fmr1*$^{+/y}$). Mice for each genotype were chosen randomly for all experiments. All mice were housed in the university's animal facility which was maintained under standard humidity and temperature with day-night cycles of 14 hr light and 10 hr darkness. Food and water were provided ad libitum. The use and care of animals in this study follows the guidelines of the UTHSCSA Institutional Animal Care and Use Committee.

BrdU Injections.

BrdU was administered through intraperitoneal injection to label proliferating GNPs in the EGL. Postnatal mice (P7 or P10) were injected with 50 mg kg^{-1} body weight of BrdU intraperitoneally 3 times (starting at P6 or P9), each 8 hr apart, and perfused with 4% PFA 8 hr after the last injection.

Brain Preparation.

Postnatal mice (P7, P10, P14, P28, P30, or adult) were anesthetized with isoflurane and perfused intracardially with PBS followed by 4% PFA (w/v) in 1X PBS. Brains were dissected out and fixed in 4% PFA for 4 hr at 4°C, and then stored in 30% sucrose

for 2 days. Brains were kept at −80°C after being embedded into embedding mold with Tissue-Plus® O.C.T. Compound. Sagittal sections (20 μm) were obtained by cryostat and collected onto a Superfrost Plus slide. The sections were stored in −20°C until used for immunostaining as previously described (Lee et al., 2020) or β-gal staining.

Immunostaining.

For immunostaining, all sections were prepared as described above (see Brain Preparation Section) and were post-fixed by methanol for 10 min at −20°C, followed by antigen retrieval for 15 min. Antigen retrieval was performed by steaming in a citrate buffer (0.294% sodium citrate, 0.05% Tween 20 in distilled water, pH 6.0) for 15 min with subsequent cooling over ice for 10 min. After being washed 3 times with PBS for 5 min, the sections were incubated for 1 hr at room temperature with blocking solution (5% goat serum and 0.01% Triton-X 100 in 1X PBS). After that, the sections were incubated with primary antibodies (aside from anti-BrdU and anti-Arl13b) overnight at 4°C. The sections were then washed 3 times with PBS for 10 min, followed by incubation with secondary antibodies for 1.5 hr at room temperature. After again being washed 3 times with PBS for 5 min, the sections were incubated with 1X DAPI for 5 min and then washed twice for 5 min. They were then incubated in 70% ethanol for 1 min before being mounted with ProLong Gold Antifade Reagent. Immunostained sections were kept in 4°C. For BrdU immunostaining, after initial primary antibody incubation, the brain tissues were washed 4 times with PBS for 10 min and incubated in 2M HCl for 30 min at 37°C before being incubated with BrdU and Arl13b primary antibodies for 4 hr at room temperature, which was then followed by washing and secondary incubation as mentioned above.

β-galactosidase (β-gal) staining.

For β-gal staining, all sections were prepared as described above (see Brain Preparation Section). β-gal activity was detected in 20 μm frozen sections by incubation in 1X X-gal solution from the X-Gal Staining Kit at 37°C for 4–6 hr unless otherwise indicated. Sections were counterstained in Nuclear Fast Red for 3 min. The sections were then washed with distilled water, followed by incubation with 75% ethanol for 1 min before being mounted with Permount Mounting Medium.

Imaging and Analysis.

For primary cilia immunostaining, images were taken in each brain region of interest by Zeiss Apotome fluorescence microscope with 40x oil objective lens, 10 μm range with 1 μm intervals. Two images were taken from the inner region (toward the inner side of the fissures where lobes are adjacent to each other, as shown in Figure 1A and 4A) of each lobe of the brain analyzed per animal (lobe V, lobe VI, lobe VIII, and lobe IX for all animals, aside from animals immunostained with NeuN, where only two images from lobe IX were taken). All 11 slices in a 10 μm thickness were counted from the region of interest (same size for all images to compare between groups) for $Arl13b^+$ primary cilia and normalized by the number of $BLBP^+$, $calbindin^+$, $NeuN^+$, or $DAPI^+$ cells. For BrdU analysis, images were taken by Zeiss Apotome fluorescence microscope with 40x oil objective lens, 10 μm range with 1 μm intervals. 4 images for P7 or 3 images for P10 were taken from the inner region (toward the inner side of the fissures where lobes are adjacent to each other, as shown in

Figure 1A and 4A) of each lobe of the brain analyzed per animal (lobe VIII and lobe IX for all animals). In 11 slices with a total 10 μm thickness, 8 slices from slice 1 to 8 were counted from the region of interest (same size for all images to compare between groups) for $BrdU^+$ and normalized by the number of $DAPI^+$ cells. For β-galactosidase staining, images were taken by N-Storm Nikon microscope with 20x objective lens. Two images were taken from the inner region (toward the inner side of the fissures where lobes are adjacent to each other, as shown in Figure 1A and 4A) of each lobe of the brain analyzed per animal (lobe VIII and lobe IX for all animals). The number of $LacZ^+$ cells in an area of 5000 μm^2 were counted and analyzed through GraphPad Prism 7.0.

Statistical Analysis.

All data was analyzed using GraphPad Prism 7.0. Significant differences were designated by student's unpaired *t*-test. For all comparisons, values of $P<0.05$ were considered significant, and all data were presented as mean ± SEM. Outliers were determined using the ROUT method with Q=0.01%. All the statistics showed that variances are similar between the groups that are being statistically compared. No statistical methods were used to pre-determine sample sizes, but all sample sizes are similar to those generally employed in the field. Sample size (n) is indicated in each figure legend. None of the samples were excluded for the analysis.

Results

Primary cilia are significantly reduced specifically in the Purkinje cell layer of the posterior cerebellum in *Fmr1* KO mice

To investigate whether adult *Fmr1* KO mice showed primary ciliary deficits, we analyzed primary cilia in various lobes of the cerebellum, specifically the anterior (defined as lobes I to V), central (defined as lobes VI to VII), and posterior (defined as lobes VIII to X) cerebellum (Reeber et al., 2012; White and Sillitoe, 2013), and in the PCL and the IGL layers, where cells express primary cilia (Figure 1A). The molecular layer (ML) was not analyzed as it consists of mostly cell processes, while the EGL has already disappeared by the third postnatal week in mice after cell migration is complete (Xu et al., 2013). Sagittal sections of cerebellum from adult WT and *Fmr1* KO mice were prepared, and immunostaining of ADP ribosylation factor-like GTPase 13b (Arl13b, red), to visualize primary cilia, and DAPI nuclear staining (grey), to visualize cells, were performed (Figure 1B). $Arl13b^+$ primary cilia were counted and normalized by the number of $DAPI^+$ cells in the PCL and the IGL layers of the anterior (lobe V), central (lobe VI), and posterior (lobes VIII/IX) cerebellum (Figure 1B) from adult WT and *Fmr1* KO mice. As a result, $Arl13b^+$ primary cilia were significantly reduced in the PCL of the posterior region of the cerebellum from adult *Fmr1* KO mice compared to WT mice, while no significant difference in primary cilia number was found in the PCL of the anterior or central regions between WT and *Fmr1* KO mice (Figure 1C: Left graph). Moreover, in the IGL, there was no significant difference in the number of primary cilia between WT and *Fmr1* KO mice in all three regions (Figure 1C: Right graph). Our results suggest that a reduction of $Arl13b^+$ is specifically seen in the PCL of the posterior cerebellum in adult *Fmr1* KO mice.

In order to check the EGL, we also analyzed primary cilia in the posterior cerebellum of WT and *Fmr1* KO mice at P7, when the EGL is still present (Figure S1). As a result, we did not find a significant reduction in primary cilia number in the EGL of the posterior region of the cerebellum in P7 *Fmr1* KO mice (Figure S1B), as well as no significant reduction in the IGL (Figure S1C). Given that our result showed a significant reduction of primary cilia in the PCL of adult *Fmr1* KO mice (Figure 1), we further checked the PCL in the anterior, central, and posterior regions of P7 mice. However, no significant reduction in primary cilia number was found in any of PCL regions of *Fmr1* KO mice compared to WT mice at age P7 (Figure S1D–S1F), implicating that primary cilia reduction in *Fmr1* KO mice is potentially age-dependent.

Primary cilia loss in *Fmr1* KO mice are cell-specific to the Bergmann glia and age-dependent in the cerebellum

Next, we determined if the phenotype observed in Figure 1 was cell type-specific among the three major cell types in the PCL, which are granule neurons, Purkinje cells, and Bergmann glia. In order to investigate primary cilia on specific cell types, we immunostained the posterior cerebellum of adult WT and *Fmr1* KO mice with the following cell markers: neuronal nuclear protein (NeuN, cyan) to visualize granule neuron, calbindin (green) to visualize Purkinje cells, or BLBP (yellow) to visualize Bergmann glia, along with Arl13b (red) and DAPI nuclear staining (grey) (Figure 2A). We then determined whether granule neurons ($NeuN^+$), Purkinje cells ($calbindin^+$), and Bergmann glia ($BLBP^+$) in the PCL of the posterior cerebellum had primary cilia ($Arl13b^+$, blue arrows) or did not have primary cilia ($Arl13b^-$, magenta arrowheads) (Figure 2A). As a result, granule neurons and Purkinje cells did not show a significant change in primary cilia number between WT and *Fmr1* KO mice, but Bergmann glia showed a significant reduction of primary cilia number in *Fmr1* KO mice compared to WT mice (Figure 2B). When immunostaining with antibodies for other cellular markers for Bergmann glia, S-100β and Sox-2, there was still a significant reduction in primary cilia number in *Fmr1* KO mice compared to WT mice (Figure S2), which confirms the reduction of primary cilia in Bergmann glia. Furthermore, Bergmann glia, marked by BLBP, S-100β, or Sox-2, as well as Purkinje cells, marked by calbindin, in both the anterior and central regions of the cerebellum in WT and *Fmr1* KO mice showed no significant difference in number of primary cilia (Figure S3). This indicates that the reduction of primary cilia in the PCL of *Fmr1* KO mice is specific to Bergmann glia in the posterior cerebellum and not in other cell types or regions of the cerebellum.

Bergmann glia are unipolar astrocytes that are associated with Purkinje cells in the PCL of the cerebellum and have unique roles both in early postnatal cerebellar development and in the mature cerebellum (Saab et al., 2012; Yamada et al., 2000). They are located directly next to Purkinje cells and interact with them in multiple ways, such as controlling Purkinje cell membrane potential (Wang et al., 2012) and regulating Purkinje cell synaptic transmission through glutamate receptors (Farmer et al., 2016; Saab et al., 2012). Importantly, Bergmann glial primary cilia perform Shh signaling by receiving Shh molecules secreted by Purkinje cells (Farmer et al., 2016). Notably, it has been previously demonstrated that altering Shh signaling in Bergmann glia has led to alterations in Bergmann glial properties making them similar to that of velate astrocytes (Farmer et al.,

2016). Other previous studies further showed that reduced Shh signaling in the Bergmann glia reduced cerebellar size, and notably, decreased cerebellar GNP proliferation in the EGL, indicating that Bergmann glia mediate neuronal-glial communications (Cheng et al., 2018; Marazziti et al., 2013). Given this neuronal-glial communication is crucial during early postnatal cerebellar development through primary cilia and Shh signaling in Bergmann glia (Cheng et al., 2018; Marazziti et al., 2013), knowing when Bergmann glia begin to lose primary cilia in *Fmr1* KO mice is critical in understanding the role of the primary cilia in the Bergmann glia to elucidate FXS pathophysiology. To investigate when the primary cilia loss in Bergmann glia begins in *Fmr1* KO mice, Arl13b^{+} primary cilia were counted and normalized by Bergmann glia population (BLBP^{+}) in the PCL of the posterior cerebellum in P7, P10, P14, P28, or adult WT or *Fmr1* KO mice (Figure 2C). As a result, while P7 animals showed no significant difference in primary cilia number between WT and *Fmr1* KO mice, P10 and older *Fmr1* KO mice showed a significant reduction in the number of primary cilia (Figure 2D), indicating that primary cilia loss in Bergmann glia of *Fmr1* KO mice occurs age-dependently. Further investigation showed that there is no significant difference in the number of Bergmann glia or Purkinje cells between genotypes in various age groups tested (Figure S4). Overall, our results demonstrate that primary cilia reduction is specifically found in Bergmann glia (cell type-specific) of the posterior cerebellum (location-specific) starting at P10 (age-specific) in *Fmr1* KO mice.

Shh signaling is reduced in Bergmann glia of *Fmr1* KO mice

Since Shh signaling and primary cilia in Bergmann glia are known to contribute to cerebellar development, such as GNP proliferation in the EGL through Shh signaling (Cheng et al., 2018; Marazziti et al., 2013), we further determined whether Shh signaling levels in Bergmann glia of *Fmr1* KO mice are altered using Gli1-*lacZ* mice, which are *lacZ* knock-in mutant mice that can be used to determine Gli1 expression levels. We performed β-galactosidase (*lacZ*) staining of the cerebellum from Gli1-*lacZ*;WT and Gli1-*lacZ*;*Fmr1* KO mice, as Gli1 is a well-defined indicator of Shh signaling and is primarily expressed in cerebellar Bergmann glia in the PCL (Corrales et al., 2004). As a result, while P7 *Fmr1* KO mice showed no significant Shh signaling changes, P10, P14, and P30 *Fmr1* KO mice demonstrated reduced Shh signaling compared to WT mice in the PCL (Figure 3). Given that Gli1 expresses mainly in Bergmann glia in the PCL and our findings showed that Bergmann glia number didn't change in various ages of *Fmr1* KO mice (Figure S4A), we conclude that Shh signaling is reduced in the Bergmann glia of *Fmr1* KO mice at P10, P14, and P30.

FMRP loss induces reductions of GNP proliferation in the EGL and the thickness of EGL

Previous studies showed that Shh signaling of Bergmann glia in the PCL is critical for the proliferation of cerebellar granule precursors in the EGL (Cheng et al., 2018; Marazziti et al., 2013). Given that a reduction of primary cilia number and Shh signaling in Bergmann glia was observed in *Fmr1* KO mice from P10 but not at P7, we next determined whether the primary cilia loss in *Fmr1* KO mice affects the proliferation of cerebellar GNPs and the thickness of the EGL (Figure 4A). In order to investigate cell proliferation in the EGL, we labeled proliferating cells using BrdU, and checked if GNP proliferation in the EGL of *Fmr1* KO mice was altered. Since the EGL is present in mice until approximately the end of the

second postnatal week and is completely depleted around P20 (Marazziti et al., 2013; Galas et al., 2017), we injected BrdU into P6 or P9 WT and *Fmr1* KO mice (3 times, 8 hr apart), and then collected the brains at P7 or P10, which was 8 hr after the last injection. As a result, at P7, there was no significant difference in the number of proliferating cells ($BrdU^+$;$DAPI^+$) in the EGL between WT and *Fmr1* KO mice (Figure 4B–C). However, at P10, the number of proliferating cells in the EGL was significantly decreased in *Fmr1* KO mice compared to WT mice (Figure 4B–C), indicating decreased proliferation of cells in the EGL of *Fmr1* KO mice compared to WT mice. Moreover, we found that the EGL thickness was reduced at P10 in *Fmr1* KO mice compared to WT mice, while no difference was observed at P7 in *Fmr1* KO mice (Figure 4D). This decrease in EGL thickness could be due to a disruption in cerebellar development led by decreased proliferation of GNPs in the EGL (Wallace, 1999). To exclude the possibility that decreased GNP proliferation is due to cilia deficits in the cerebellar GNPs of the EGL as a previous study has demonstrated (Chang et al., 2019), we counted the number of primary cilia in the EGL of WT and *Fmr1* KO mice and found no significant difference between WT and *Fmr1* KO mice (Figure 4E), indicating that the primary cilia loss in the Bergmann glia of *Fmr1* KO mice is what affects GNP proliferation and the thickness of EGL in *Fmr1* KO mice. These results demonstrate that reduction of Shh signaling due to the primary cilia loss in the Bergmann glia of *Fmr1* KO mice causes decreased proliferation of GNPs in the EGL.

Discussion

Defective primary cilia have been associated with diverse human diseases including Bardet-Biedl, Joubert, Meckel-Gruber and Oral-facial-digital type 1 syndromes (Badano et al., 2006). The pathology of these disorders known as ciliopathies include neurodevelopmental deficits and cognitive defects, suggesting that primary cilia are required for the proper development or function of the brain. Despite this growing evidence of primary cilia contribution to brain development and intellectual disabilities, the functional role of primary cilia in neurodevelopmental disorders, such as FXS, is largely unknown. FXS patients have a range of developmental deficits, such as cognitive impairment and intellectual disabilities, and also display cerebellar behavioral phenotypes (Bardoni et al., 2006; Greco et al., 2011; O'Donnell and Warren, 2002). *Fmr1* KO mice, a mouse model for FXS, recapitulate human behavioral deficits including cerebellar deficits (Roy et al., 2011); notably, deficits in synaptic structure, plasticity, and eye-blink conditioning behavior were observed when FMRP was conditionally knocked out in Purkinje cells of the cerebellum, indicating that the altered plasticity or function of the cerebellum could be the cause of FXS phenotypes (Koekkoek et. al. 2005). In this report, we demonstrate that primary cilia loss and Shh signaling reduction are found in the cerebellar Bergmann glia of *Fmr1* KO mice. This finding suggests a link between primary cilia and FXS, as well as provides a novel cellular phenotype of Bergmann glia in the condition of FMRP loss. The cerebellum has recently emerged as one of the key brain regions affected in autism, and anatomical, clinical, and neuroimaging studies strongly suggest that the cerebellum supports cognitive functions, including language and executive functions (Becker and Stoodley, 2013). Interestingly, our result shows that primary cilia deficits are detected in the posterior region of the cerebellum in *Fmr1* KO mice, which correlates with previous studies demonstrating panfoliar atrophy

and decreased size of the cerebellar vermis in the posterior region of the cerebellum in FXS patients (Greco et al., 2011; Reiss et al., 1988). Notably, damage or deficit to the posterior region of the cerebellum has been linked to cognitive deficits such as memory and language, whereas the anterior and central regions have been found to have a greater effect on motor control (Stoodley and Schmahmann, 2010; Stoodley et. al., 2012). The cognitive deficits seen in FXS are consistent with the behaviors mediated by the posterior cerebellum. Our results also demonstrate the ciliary loss in cerebellar Bergmann glia, which suggest a potential contribution of primary cilia deficits to cerebellar phenotypes of FXS through neuronal-glial communications. Together with our recent report demonstrating primary cilia deficits in the newborn neurons from dentate gyrus of *Fmr1* KO mice (Lee et al., 2020), primary cilia can be proposed as a potential contributor in the development of postnatal born neurons in both cerebellum and dentate gyrus of FXS. Elucidating the further mechanisms underlying this contribution of primary cilia loss to FXS pathophysiology can be a potential future study that can fill our current knowledge gap.

Bergmann glia are specialized astrocytic cells in the cerebellum, and are a close anatomical partner to Purkinje cells (Bellamy, 2006). Bergmann glia contribute to Purkinje cell dendritic elaboration by synapsing on Purkinje cell dendrites (Lippman et al., 2008; Yamada et al., 2000) and by receiving Shh signaling from Purkinje cells (Farmer et al., 2016). In early postnatal cerebellar development, Bergmann glia extend processes upward through the ML to the EGL and end at the pial surface to provide structural support and guide the migration of granule neurons from the EGL to the IGL (Xu et al., 2013). More recently, Bergmann glia were found to regulate the proliferation of cerebellar GNPs in the EGL through Shh signaling via primary cilia (Cheng et al., 2018; Marazziti et al., 2013). Therefore, our finding of both primary cilia reduction and Shh signaling reduction specifically in the Bergmann glia implies deficits in Bergmann glia function, which may have led to altered interactions with GNPs in the EGL. Since Gli1, a Shh signaling product found in Bergmann glia, is known to be downregulated soon after GNPs differentiate (Corrales et al., 2004), this implies that the reduced thickness of the EGL in *Fmr1* KO mice at P10 may be caused by early differentiation of the GNPs due to altered communication with Bergmann glia through Shh signaling. Given that we found a novel cellular deficit in the cerebellum of *Fmr1* KO mice, revealing the underlying molecular mechanism of how FMRP ablation leads to reduced primary cilia in the Bergmann glia and how this phenotype contributes to an EGL phenotype (reduced GNP proliferation and thickness) in *Fmr1* KO mice can be a potential follow up study. Given that FMRP is an mRNA-binding protein that associates with polyribosomes and regulates the trafficking, stability, and translation of mRNA (Laggerbauer et al., 2001; Lee et al., 2011), one potential scenario might be that FMRP may contribute to this primary cilia phenotype directly or indirectly by regulating mRNAs, which are critical for primary ciliogenesis. The molecular mechanisms underlying primary cilia deficits in Bergmann glia of FXS can be further investigated by identifying FMRP mRNA targets and characterizing how FMRP regulates primary cilia.

Conclusion

This study pursued finding a phenotype of primary cilia in the cerebellum using *Fmr1* KO mice. The initial investigation assessed the number of primary cilia in different regions of

the cerebellum (anterior, central, and posterior) in the PCL and the IGL of WT and *Fmr1* KO adult mice. Our results demonstrate that primary cilia reduction is specifically found in Bergmann glia (cell type-specific) of the posterior cerebellum (location-specific) starting at P10 (age-specific) in *Fmr1* KO mice. We further observed the reduction of Gli1 expression, an indicator of Shh signaling in Bergmann glia, and the reduction of GNP proliferation and thickness in the EGL in *Fmr1* KO mice without observing a change in primary cilia number in the EGL. Given that Shh signaling in Bergmann glia plays a critical role in GNP proliferation in the EGL, our results indicate that dysregulated Shh signaling in Bergmann glia through primary cilia in *Fmr1* KO mice may have led to the reduced proliferation of GNPs and, therefore, the reduced thickness of the EGL observed. In conclusion, we demonstrate that FMRP is required for primary cilia on the Bergmann glia for proper development of the cerebellum possibly through glia-neuronal communication.

Supplementary Material

Refer to Web version on PubMed Central for supplementary material.

Acknowledgements

We thank Exing Wang for technical support on imaging and Daisy Brockhouse for assisting with analysis.

Funding

This work was supported by the National Institute of Mental Health (R01MH125979), the National Institute on Aging (R21AG072423), the UT Rising STARs award, and the Simons Foundation Autism Research Initiative (SFARI) pilot award (#574967).

Data Availability

All data that support the findings of this study are available from the corresponding author upon reasonable request.

References

Aksoy A, Karaguzel G, Akbulut U, and Turk A (2011). Two sisters with Bardet-Biedl syndrome: brain abnormalities and unusual facial findings. Turk J Pediatr 53, 460–463. [PubMed: 21980853]

Antar LN, Afroz R, Dictenberg JB, Carroll RC, and Bassell GJ (2004). Metabotropic glutamate receptor activation regulates fragile x mental retardation protein and FMR1 mRNA localization differentially in dendrites and at synapses. J Neurosci 24, 2648–2655. [PubMed: 15028757]

Badano JL, Mitsuma N, Beales PL, and Katsanis N (2006). The ciliopathies: an emerging class of human genetic disorders. Annu Rev Genomics Hum Genet 7, 125–148. [PubMed: 16722803]

Bakker CE, de Diego Otero Y, Bontekoe C, Raghoe P, Luteijn T, Hoogeveen AT, Oostra BA, and Willemsen R (2000). Immunocytochemical and biochemical characterization of FMRP, FXR1P, and FXR2P in the mouse. Exp Cell Res 258, 162–170. [PubMed: 10912798]

Bardoni B, Davidovic L, Bensaid M, and Khandjian EW (2006). The fragile X syndrome: exploring its molecular basis and seeking a treatment. Expert Rev Mol Med 8, 1–16.

Becker EB, and Stoodley CJ (2013). Autism spectrum disorder and the cerebellum. Int Rev Neurobiol 113, 1–34. [PubMed: 24290381]

Bellamy TC (2006). Interactions between Purkinje neurones and Bergmann glia. Cerebellum 5, 116–126. [PubMed: 16818386]

Breunig JJ, Sarkisian MR, Arellano JI, Morozov YM, Ayoub AE, Sojitra S, Wang B, Flavell RA, Rakic P, and Town T (2008). Primary cilia regulate hippocampal neurogenesis by mediating sonic hedgehog signaling. Proc Natl Acad Sci U S A 105, 13127–13132. [PubMed: 18728187]

Chang CH, Zanini M, Shirvani H, Cheng JS, Yu H, Feng CH, Mercier AL, Hung SY, Forget A, Wang CH, et al. (2019). Atoh1 Controls Primary Cilia Formation to Allow for SHH-Triggered Granule Neuron Progenitor Proliferation. Dev Cell 48, 184–199 e185. [PubMed: 30695697]

Cheng FY, Fleming JT, and Chiang C (2018). Bergmann glial Sonic hedgehog signaling activity is required for proper cerebellar cortical expansion and architecture. Dev Biol 440, 152–166. [PubMed: 29792854]

Chizhikov VV, Davenport J, Zhang Q, Shih EK, Cabello OA, Fuchs JL, Yoder BK, and Millen KJ (2007). Cilia proteins control cerebellar morphogenesis by promoting expansion of the granule progenitor pool. J Neurosci 27, 9780–9789. [PubMed: 17804638]

Cook D, Sanchez-Carbente M.e.R., Lachance C, Radzioch D, Tremblay S, Khandjian EW, DesGroseillers L, and Murai KK (2011). Fragile X related protein 1 clusters with ribosomes and messenger RNAs at a subset of dendritic spines in the mouse hippocampus. PLoS One 6, e26120. [PubMed: 22022532]

Corrales JD, Rocco GL, Blaess S, Guo Q, and Joyner AL (2004). Spatial pattern of sonic hedgehog signaling through Gli genes during cerebellum development. Development 131, 5581–5590. [PubMed: 15496441]

Di Pietro C, Marazziti D, La Sala G, Abbaszadeh Z, Golini E, Matteoni R, and Tocchini-Valentini GP (2017). Primary Cilia in the Murine Cerebellum and in Mutant Models of Medulloblastoma. Cell Mol Neurobiol 37, 145–154. [PubMed: 26935062]

Farmer WT, Abrahamsson T, Chierzi S, Lui C, Zaelzer C, Jones EV, Bally BP, Chen GG, Theroux JF, Peng J, et al. (2016). Neurons diversify astrocytes in the adult brain through sonic hedgehog signaling. Science 351, 849–854. [PubMed: 26912893]

Feng Y, Gutekunst CA, Eberhart DE, Yi H, Warren ST, and Hersch SM (1997). Fragile X mental retardation protein: nucleocytoplasmic shuttling and association with somatodendritic ribosomes. J Neurosci 17, 1539–1547. [PubMed: 9030614]

Flora A, Klisch TJ, Schuster G, and Zoghbi HY (2009). Deletion of Atoh1 disrupts Sonic Hedgehog signaling in the developing cerebellum and prevents medulloblastoma. Science 326, 1424–1427. [PubMed: 19965762]

Galas L, Benard M, Lebon A, Komuro Y, Schapman D, Vaudry H, Vaudry D, and Komuro H (2017). Postnatal Migration of Cerebellar Interneurons. Brain Sci 7.

Giovannucci A, Badura A, Deverett B, Najafi F, Pereira TD, Gao Z, Ozden I, Kloth AD, Pnevmatikakis E, Paninski L, et al. (2017). Cerebellar granule cells acquire a widespread predictive feedback signal during motor learning. Nat Neurosci 20, 727–734. [PubMed: 28319608]

Greco CM, Navarro CS, Hunsaker MR, Maezawa I, Shuler JF, Tassone F, Delany M, Au JW, Berman RF, Jin LW, et al. (2011). Neuropathologic features in the hippocampus and cerebellum of three older men with fragile X syndrome. Mol Autism 2, 2. [PubMed: 21303513]

Han YG, Spassky N, Romaguera-Ros M, Garcia-Verdugo JM, Aguilar A, Schneider-Maunoury S, and Alvarez-Buylla A (2008). Hedgehog signaling and primary cilia are required for the formation of adult neural stem cells. Nat Neurosci 11, 277–284. [PubMed: 18297065]

Huang CC, Sugino K, Shima Y, Guo C, Bai S, Mensh BD, Nelson SB, and Hantman AW (2013). Convergence of pontine and proprioceptive streams onto multimodal cerebellar granule cells. Elife 2, e00400. [PubMed: 23467508]

Huangfu D, Liu A, Rakeman AS, Murcia NS, Niswander L, and Anderson KV (2003). Hedgehog signalling in the mouse requires intraflagellar transport proteins. Nature 426, 83–87. [PubMed: 14603322]

Koekkoek SK, Yamaguchi K, Milojkovic BA, Dortland BR, Ruigrok TJ, Maex R, De Graaf W, Smit AE, VanderWerf F, Bakker CE, et al. (2005). Deletion of FMR1 in Purkinje cells enhances parallel fiber LTD, enlarges spines, and attenuates cerebellar eyelid conditioning in Fragile X syndrome. Neuron 47, 339–352. [PubMed: 16055059]

Lackey EP, Heck DH, and Sillitoe RV (2018). Recent advances in understanding the mechanisms of cerebellar granule cell development and function and their contribution to behavior. F1000Res 7.

Laggerbauer B, Ostareck D, Keidel EM, Ostareck-Lederer A, and Fischer U (2001). Evidence that fragile X mental retardation protein is a negative regulator of translation. Hum Mol Genet 10, 329–338. [PubMed: 11157796]

Lee HY, Ge WP, Huang W, He Y, Wang GX, Rowson-Baldwin A, Smith SJ, Jan YN, and Jan LY (2011). Bidirectional regulation of dendritic voltage-gated potassium channels by the fragile X mental retardation protein. Neuron 72, 630–642. [PubMed: 22099464]

Lee JH, and Gleeson JG (2010). The role of primary cilia in neuronal function. Neurobiol Dis 38, 167–172. [PubMed: 20097287]

Lee B, Panda S, and Lee HY (2020). Primary Ciliary Deficits in the Dentate Gyrus of Fragile X Syndrome. Stem Cell Reports 15, 454–466. [PubMed: 32735823]

Lippman JJ, Lordkipanidze T, Buell ME, Yoon SO, and Dunaevsky A (2008). Morphogenesis and regulation of Bergmann glial processes during Purkinje cell dendritic spine ensheathment and synaptogenesis. Glia 56, 1463–1477. [PubMed: 18615636]

Mancini F, Romani M, Micalizzi A, and Valente EM (2014). Molecular Genetics of Joubert Syndrome.

Manzini MC, Ward MS, Zhang Q, Lieberman MD, and Mason CA (2006). The stop signal revised: immature cerebellar granule neurons in the external germinal layer arrest pontine mossy fiber growth. J Neurosci 26, 6040–6051. [PubMed: 16738247]

Marazziti D, Di Pietro C, Golini E, Mandillo S, La Sala G, Matteoni R, and Tocchini-Valentini GP (2013). Precocious cerebellum development and improved motor functions in mice lacking the astrocyte cilium-, patched 1-associated Gpr37l1 receptor. Proc Natl Acad Sci U S A 110, 16486–16491. [PubMed: 24062445]

O'Donnell WT, and Warren ST (2002). A decade of molecular studies of fragile X syndrome. Annu Rev Neurosci 25, 315–338. [PubMed: 12052912]

Parisi MA (2019). The molecular genetics of Joubert syndrome and related ciliopathies: The challenges of genetic and phenotypic heterogeneity. Transl Sci Rare Dis 4, 25–49. [PubMed: 31763177]

Reiss AL, Patel S, Kumar AJ, and Freund L (1988). Preliminary communication: neuroanatomical variations of the posterior fossa in men with the fragile X (Martin-Bell) syndrome. Am J Med Genet 31, 407–414. [PubMed: 3232704]

Reeber SL, White JJ, George-Jones NA, and Sillitoe RV (2012). Architecture and development of olivocerebellar circuit topography. Front Neural Circuits 6, 115. [PubMed: 23293588]

Roy S, Zhao Y, Allensworth M, Farook MF, LeDoux MS, Reiter LT, and Heck DH (2011). Comprehensive motor testing in Fmr1-KO mice exposes temporal defects in oromotor coordination. Behav Neurosci 125, 962–969. [PubMed: 22004265]

Saab AS, Neumeyer A, Jahn HM, Cupido A, Simek AA, Boele HJ, Scheller A, Le Meur K, Gotz M, Monyer H, et al. (2012). Bergmann glial AMPA receptors are required for fine motor coordination. Science 337, 749–753. [PubMed: 22767895]

Spassky N, Han YG, Aguilar A, Strehl L, Besse L, Laclef C, Ros MR, Garcia-Verdugo JM, and Alvarez-Buylla A (2008). Primary cilia are required for cerebellar development and Shh-dependent expansion of progenitor pool. Dev Biol 317, 246–259. [PubMed: 18353302]

Stoodley CJ, Schmahmann JD (2010). Evidence for topographic organization in the cerebellum of motor control versus cognitive and affective processing. Cortex 46, 831–844. [PubMed: 20152963]

Stoodley CJ, Valera EM, Schmahmann JD (2012). Functional topography of the cerebellum for motor and cognitive tasks: an fMRI study. 59, 1560–1570

Valente EM, Rosti RO, Gibbs E, and Gleeson JG (2014). Primary cilia in neurodevelopmental disorders. Nat Rev Neurol 10, 27–36. [PubMed: 24296655]

Veland IR, Awan A, Pedersen LB, Yoder BK, and Christensen ST (2009). Primary cilia and signaling pathways in mammalian development, health and disease. Nephron Physiol 111, p39–53. [PubMed: 19276629]

Wallace VA (1999). Purkinje-cell-derived Sonic hedgehog regulates granule neuron precursor cell proliferation in the developing mouse cerebellum. Curr Biol 9, 445–448. [PubMed: 10226030]

Wang F, Xu Q, Wang W, Takano T, and Nedergaard M (2012). Bergmann glia modulate cerebellar Purkinje cell bistability via Ca2+-dependent K+ uptake. Proceedings of the National Academy of Sciences 109, 7911–7916.

Ware SM, Aygun MG, and Hildebrandt F (2011). Spectrum of clinical diseases caused by disorders of primary cilia. Proc Am Thorac Soc 8, 444–450. [PubMed: 21926397]

Watanabe M, and Kano M (2011). Climbing fiber synapse elimination in cerebellar Purkinje cells. Eur J Neurosci 34, 1697–1710. [PubMed: 22103426]

Waters AM, and Beales PL (2011). Ciliopathies: an expanding disease spectrum. Pediatr Nephrol 26, 1039–1056. [PubMed: 21210154]

Wheway G, Nazlamova L, and Hancock JT (2018). Signaling through the Primary Cilium. Front Cell Dev Biol 6, 8. [PubMed: 29473038]

White JJ, and Sillitoe RV (2013). Development of the cerebellum: from gene expression patterns to circuit maps. Wiley Interdiscip Rev Dev Biol 2, 149–164. [PubMed: 23799634]

Xu H, Yang Y, Tang X, Zhao M, Liang F, Xu P, Hou B, Xing Y, Bao X, and Fan X (2013). Bergmann glia function in granule cell migration during cerebellum development. Mol Neurobiol 47, 833–844. [PubMed: 23329344]

Yamada K, Fukaya M, Shibata T, Kurihara H, Tanaka K, Inoue Y, and Watanabe M (2000). Dynamic transformation of Bergmann glial fibers proceeds in correlation with dendritic outgrowth and synapse formation of cerebellar Purkinje cells. J Comp Neurol 418, 106–120. [PubMed: 10701759]

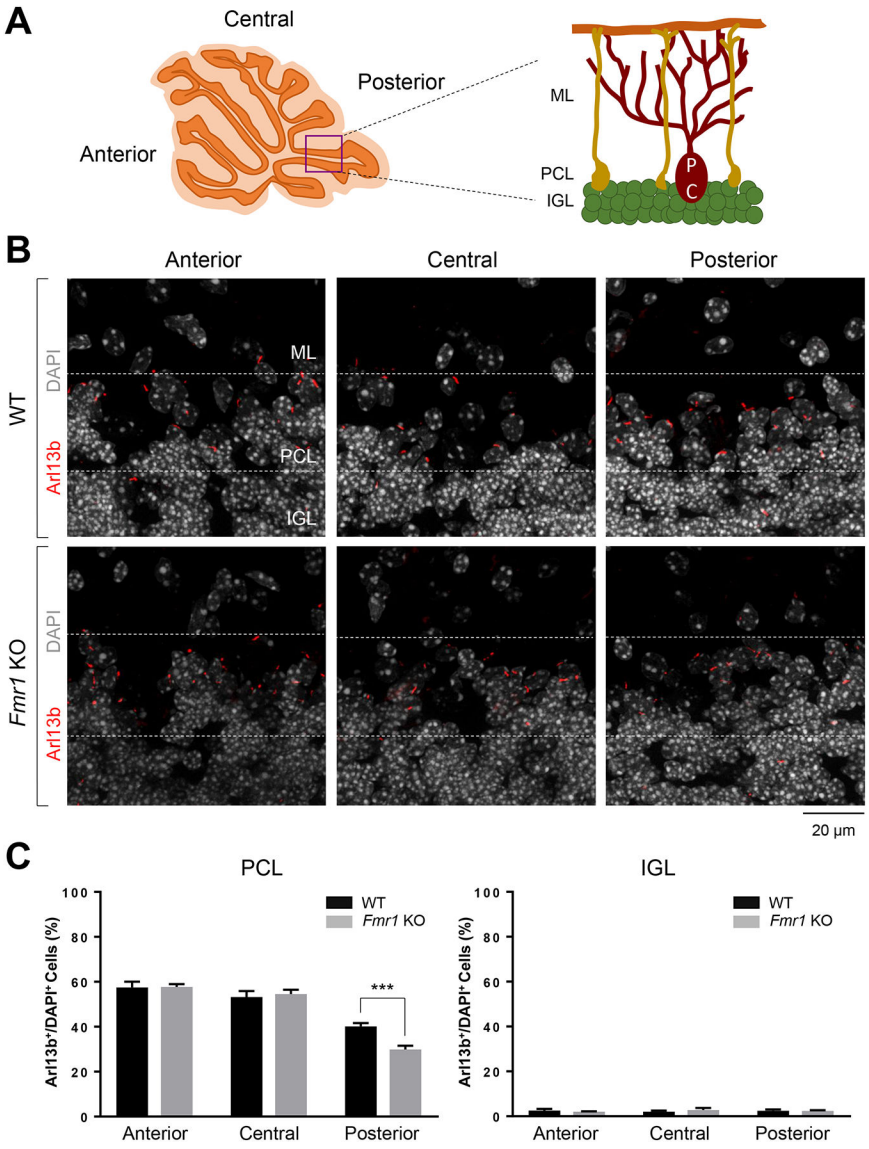

Figure 1. Number of primary cilia is reduced specifically in the Purkinje cell layer of the posterior cerebellum in adult *Fmr1* KO mice. See also Figure S1.

(A) Schematic of adult cerebellum regions and layers. (B) Immunostaining of Arl13b (*red*) with DAPI nuclear staining (*grey*) in the PCL and IGL of the anterior (left), central (middle), and posterior (right) cerebellum of adult WT (top) and *Fmr1* KO (bottom) mice. Dotted white lines indicate the borderline of each layer (ML, PCL and IGL). Scale bar, 20 μm. (C) Quantification of the percentage of $Arl13b^+$ cells among $DAPI^+$ cells in the PCL (left) or IGL (right) of the cerebellum from adult WT and *Fmr1* KO mice. n=4–8 for each group, mean ± SEM. Student's unpaired *t*-test. ***P<0.001.

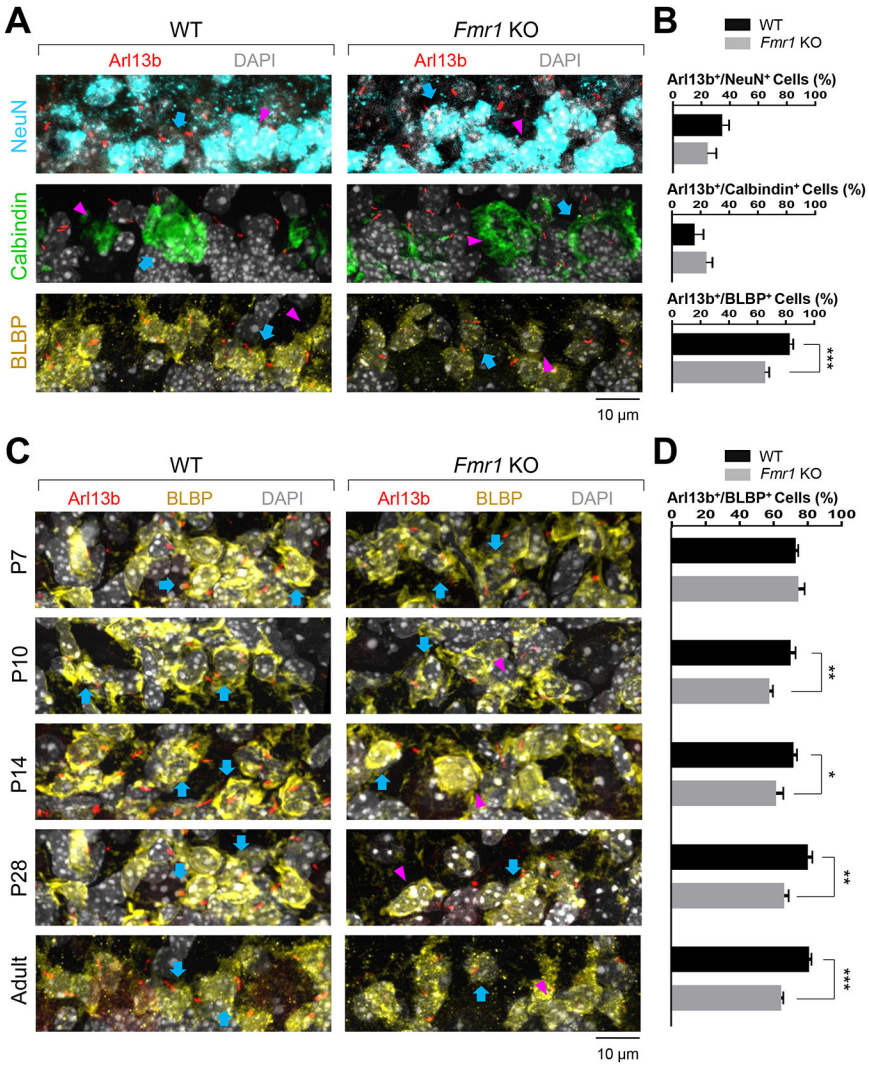

Figure 2. Number of primary cilia is reduced specifically in Bergmann glia in the posterior cerebellum of adult *Fmr1* KO mice, and significant reduction in primary cilia number starts at P10. See also Figure S2, S3, and S4.

(A) Immunostaining of Arl13b (*red*), NeuN (*cyan*, top), calbindin (*green*, middle), and BLBP (*yellow*, bottom) with DAPI nuclear staining (*grey*) in the posterior cerebellum of adult WT (left) and *Fmr1* KO (right) mice. Blue arrows, Arl13b$^+$ cells; Magenta arrowheads, Arl13b$^-$ cells. Scale bar, 10 μm. (B) Quantification of the percentage of Arl13b$^+$ cells among NeuN$^+$ cells (top), calbindin$^+$ cells (middle), or BLBP$^+$ cells (bottom) in the cerebellum from adult WT and *Fmr1* KO mice. (C) Immunostaining of Arl13b (*red*) and BLBP (*yellow*) with DAPI nuclear staining (*grey*) in the PCL of P7, P10, P14, P28, and adult WT (left) and *Fmr1* KO (right) mice. Blue arrows, Arl13b$^+$ cells; Magenta arrowheads, Arl13b$^-$ cells. Scale bar, 10 μm. (D) Quantification of the percentage of Arl13b$^+$ cells among BLBP$^+$ cells in the cerebellum from WT and *Fmr1* KO mice. n=4–8 for each group (A), n=8–24 for each group (C), mean ± SEM. Student's unpaired *t*-test. *P<0.05; **P<0.01; ***P<0.001.

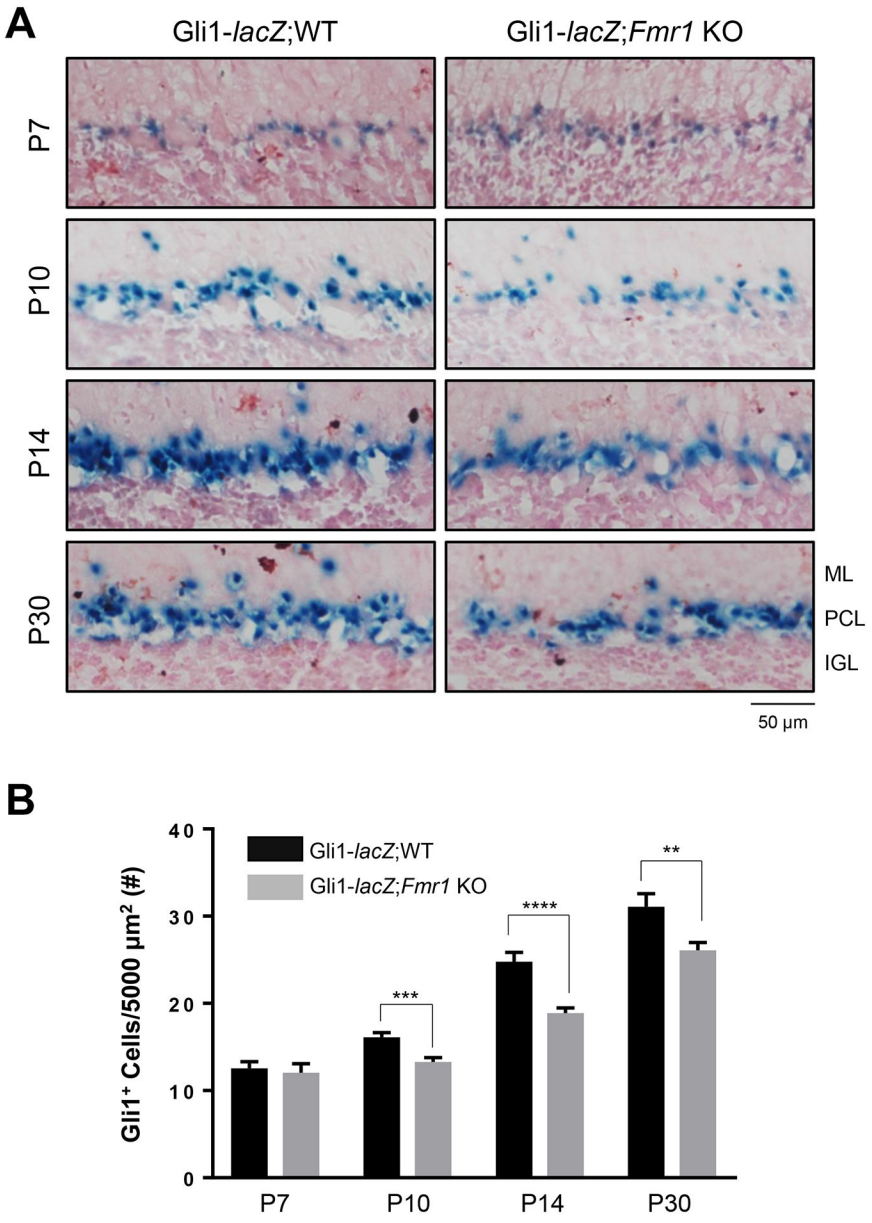

Figure 3. Shh signaling is reduced in the Bergmann glia of *Fmr1* KO mice starting at P10. See also Figure S4.

(A) β-galactosidase staining (*blue*) and nuclear staining (*red*) of the PCL in the cerebellum from Gli1-*lacZ*;WT (left) and Gli1-*lacZ*;*Fmr1* KO (right) mice at P7, P10, P14, and P30. Scale bar, 50 μm. (B) Quantification of the number of β-galactosidase^{+} cells in region of interest in square microns (μm^2). n=24–48 for each group, mean ± SEM. Student's unpaired *t*-test. **P<0.01; ***P<0.001; ****P<0.0001.

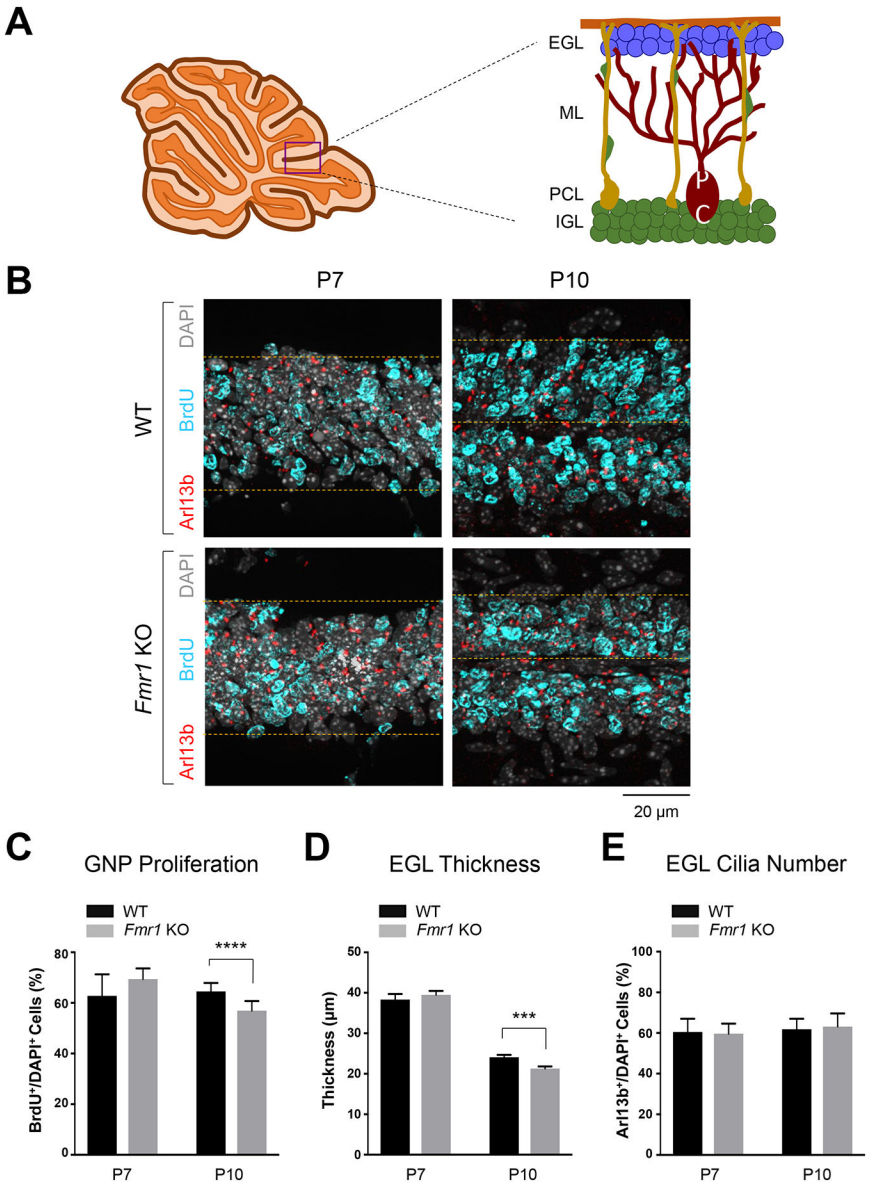

Figure 4. GNP proliferation in the EGL and thickness of EGL are reduced in the posterior cerebellum of *Fmr1* KO mice at P10.

(A) Schematic of location analyzed in the posterior cerebellum. (B) Immunostaining of Arl13b (*red*) and BrdU (*cyan*) and DAPI nuclear staining (*grey*) in the EGL of WT (top) and *Fmr1* KO (bottom) mice at P7 and P10. Dotted yellow lines indicate the borderline of EGL from one lobe. Scale bar, 20 μm. (C) Quantification of the percentage of $BrdU^+$ cells among $DAPI^+$ cells in the EGL from WT and *Fmr1* KO mice. (D) Measurement of the thickness of the EGL in microns (μm) from WT and *Fmr1* KO mice. (E) Quantification of the percentage of $Arl13b^+$ cells among $DAPI^+$ cells in the EGL from WT and *Fmr1* KO mice. n=6–9 for each group (C, E), n=2–3 for each group (D), mean ± SEM. Student's unpaired *t*-test. ***P<0.001; ****P<0.0001.